Proton Affinity of Peroxyacetyl Nitrate (PAN)

Charles E. Miller*

Department of Chemistry, Haverford College, Haverford, Pennsylvania 19041-1392

Joseph S. Francisco[†]

Department of Chemistry and Department of Earth and Atmospheric Science, Purdue University, West Lafayette, Indiana 47907-1393

Received: August 23, 2000

Ab initio calculations for the proton affinity of peroxyacetyl nitrate (PAN) reveal the complicated protonation chemistry associated with the unusual multifunctional structure of this molecule. Optimized molecular structures, relative energies, decomposition energies, and proton affinities have been determined for four chemically distinguishable $PANH^+$ protomers. Calculations performed at the CBS-Q level of theory predict that the most stable structure is the peracetic acid-nitronium ion complex, $[CH_3C(O)OOH\cdots NO_2^+]$, and yield $PA^{0\,K}_{CBS\text{-}Q}(PAN) = -773.4 \pm 10$ kJ mol^{-1}. This result disagrees with the experimental determination of $PA^{298\,K}(PAN) = -798 \pm 12$ kJ mol^{-1} that was attributed to protonation of the carbonyl oxygen but agrees with the experimental and theoretical results for the proton affinities of the nitrates $HONO_2$, CH_3ONO_2, $C_2H_5ONO_2$, and $HOONO_2$, where the most stable protomers are also of the form $[ROH\cdots NO_2^+]$.

Introduction

Peroxyacetyl nitrate (**1**, PAN) plays an important role in the global distribution of tropospheric ozone through the long-range transport of NO_x.[1] The influence of PAN on air quality has generated considerable interest in accurate real-time measurement of PAN concentrations in ambient air. Most detection schemes have implemented some variation of gas chromatography to isolate PAN from the air sample;[2,3] however, these methods require too much time to respond to the rapid changes in PAN concentration that occur near ground level. Mass spectrometric methods have the potential to provide real-time parts per trillion level PAN detection,[4−7] but there remain fundamental uncertainties surrounding the ion chemistry of PAN.

The unusual consecutive bonding of acetyl, peroxy, and nitrate functionalities in PAN produces a complicated chemical environment. The competition for electron density among the five electronegative atoms in the peroxynitrate linkage creates weak chemical bonds at both the nitrate (N_2-O_4) and peroxide (O_4-O_5) positions. This results in two low energy decomposition channels

$$CH_3C(O)OONO_2 \rightarrow CH_3C(O)OO^\bullet + NO_2 \qquad \text{(R1a)}$$

$$\rightarrow CH_3C(O)O^\bullet + NO_3 \qquad \text{(R1b)}$$

Only channel (R1a) has been observed in thermal decomposition experiments, suggesting a substantial barrier to decomposition via (R1b)[8−11] and that PAN behaves as a nitrate under these conditions. Mazely et al.[12,13] have observed significant quantum yields from both channels (R1a) and (R1b) in photodissociation experiments, demonstrating that PAN photochemistry exhibits nitrate *and* peroxide characteristics. Srinivasan et al.[5] recently reported an experimental proton affinity measurement $PA^{298\,K}(PAN) = -798 \pm 12$ kJ mol^{-1}, which they attributed to protonation at the carbonyl oxygen, indicating that PAN behaves as an acetyl molecule in ionic environments.

These markedly different chemical results prompt the question: Is PAN an acetyl, a peroxide, or a nitrate? We attack this question by noting the 50 kJ mol^{-1} discrepancy between $PA^{298\,K}(PAN)$ and the proton affinities of other nitric acid derivatives: $PA^{298\,K}(HNO_3) = -761.5 \pm 9.6$ kJ mol^{-1},[14−18] $PA^{298\,K}(CH_3ONO_2) = -745 \pm 8.4$ kJ mol^{-1},[14−18] $PA^{298\,K}(C_2H_5ONO_2) = -746.4 \pm 11$ kJ mol^{-1},[19] and $PA^{298\,K}(HOONO_2) = -736.4 \pm 12$ kJ mol^{-1}.[20] Additionally, these previous studies have shown that an accurate determination of nitrate proton affinities is complicated by the presence of multiple stable protomers with different kinetic behavior. This problem is compounded in PAN where there are four chemically distinguishable oxygen atom sites, all of which should support stable protomers. The determination of which oxygen atom site produces the most stable PAN protomer (i.e., which oxygen atom is the most basic) will help confirm the chemical identity of PAN. Furthermore, a complete understanding of $PANH^+$ chemistry is crucial to the design of chemical ionization techniques to monitor PAN.

Results

A detailed description of the computational methods employed in this study has been given previously.[11] All calculations were performed using the Gaussian 98 program suite.[21] Optimized molecular structures were computed using the Becke3-Lee−Yang−Parr (B3LYP) density functional[22] and the basis sets 6-31G* through 6-311++G(3df,3pd).[23−29] Thermochemical calculations employed the ab initio complete basis set (CBS) model chemistries CBS-4[30] and CBS-Q[30] as well as the G2-(MP2) method.[31]

Our previous work on the thermal dissociation of PAN[11] suggests that the ab initio model chemistries will yield chemically accurate proton $PA^{298\,K}(PAN)$ values. To confirm this assumption, we calculated the proton affinities for a series of molecules containing the nitrate and carbonyl functional groups. Table 1 compares the model chemistry proton affinities for these

---

* To whom correspondence should be addressed. E-mail: cmiller@haverford.edu.

[†] E-mail: jfrancis@chem.purdue.edu.

10.1021/jp0030185 CCC: $20.00

TABLE 1: Ab Initio Energies (hartrees) and Proton Affinities (kJ mol^{-1}) for the Test Set Molecules

	B3LYP/6-311(3df,3pd)	G2(MP2)	CBS-4	CBS-Q	theory	expt
HNO_3	−281.00018	−280.55010	−280.59556	−280.57585		
$[H_2O\cdots NO_2^+]$	−281.28986	−280.83834	−280.87199	−280.86126		
PA(HNO_3) (kJ mol^{-1})	−760.4	−756.6	−725.6	−749.2	−763.6[a]	−761.5[b]
CH_3ONO_2	−320.31781	−319.76422	−319.81905	−319.79030		
$[CH_3OH\cdots NO_2^+]$	−320.60551	−320.04518	−320.07929	−320.06834		
PA(CH_3ONO_2) (kJ mol^{-1})	−755.2	−737.5	−683.1	−729.9	−739.3[a]	−732.2[c]
$[H_2COH]^+$	−114.83180	−114.60531	−114.62413	−114.61068		
H_2CO	−114.54994	−114.33607	−114.35829	−114.34272		
PA(H_2CO) (kJ mol^{-1})	−703.5	−706.8	−697.8	−703.4	−711.8[d] −706.7[e] −713.4[f]	−718.4[g]
$[CH_3CHOH]^+$	−154.19948	−153.86360	−153.89685	−153.87036		
CH_3CHO	−153.89333	−153.57297	−153.60933	−153.58082		
PA(CH_3CHO) (kJ mol^{-1})	−748.8	−762.9	−754.7	−760.1	−770.2[d] −770.8[d]	−768[g]
$[CH_3C(OH)CH_3]^+$	−193.55626	−193.11624	−193.16445	−193.12478		
$CH_3C(O)CH_3$	−193.23232	−192.8089	−192.85938	−192.81837		
PA($CH_3C(O)CH_3$) (kJ mol^{-1})	−850.3	−806.8	−800.8	−804.3	−811.9[d] −812.7[d]	−810[g]

[a] Ref 15. [b] Ref 13. [c] Ref 14. [d] Ref 30. [e] Ref 31. [f] Ref 32. [g] Ref 33.

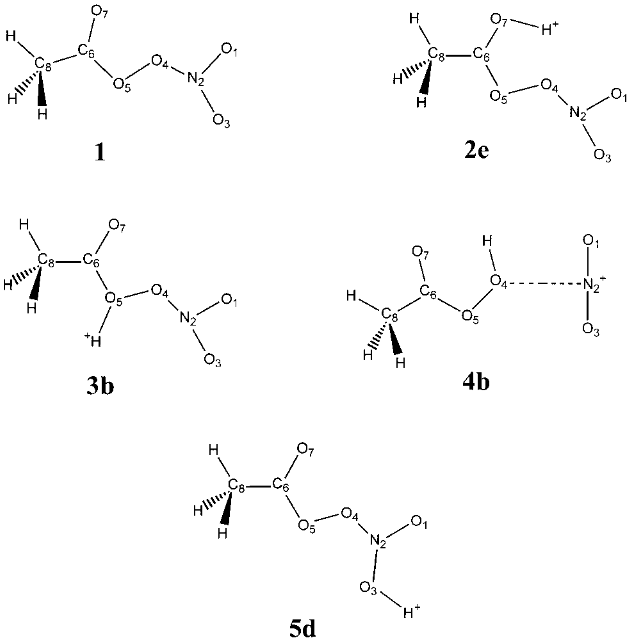

1 **2e** **3b** **4b** **5d**

Figure 1. Optimized structures for PAN and minimum energy PANH$^+$ protomers.

compounds to experimental and theoretical values taken from the literature.[15−17,32−35] We conclude from this exercise that the CBS-Q and G2(MP2) methods reproduce the proton affinities for PAN-like molecules within the 10 kJ mol^{-1} uncertainty limits expected for these model chemistries.[30,31] The CBS-4 results display significantly larger errors.

Exploratory calculations identified stable PANH$^+$ structures corresponding to protonation at the carbonyl oxygen atom (**2**), the peroxy oxygen atom (**3**), the nitrate oxygen atom (**4**), and the terminal oxygen atoms (**5**). Identifying the minimum energy structures for **2**−**5** is not trivial because multiple rotational conformers exist for each protomer even though the heavy atom framework preferentially maintains a planar configuration. Additional calculations were conducted at the B3LYP/6-31G(d) level of theory to obtain the minimum energy structure for each protomer. These calculations were conducted by fixing the crucial dihedral angles in a specified configuration and freely optimizing all other structural parameters. The dihedral angles were constrained to 0°, 90°, or 180° because these values generally preserve the planarity of the heavy atom frame. The minimum energy rotomers for PAN and each PANH$^+$ protomer are depicted in Figure 1; Table 2 presents the corresponding energies and Table 3 gives the vibrational frequencies. The coordinates of the optimized structures for all rotomers are available from the authors upon request.

TABLE 2: Conformational Analysis of PANH$^+$ Protomers at the B3LYP/6-31G(d) Level of Theory

protomer	τ_1, τ_2, τ_3	energy
2a	cis−cis−cis	−508.97540
2b	trans−cis−cis	−508.96853
2c	cis−trans−trans	−508.96974
2d	trans−trans−cis	−508.96627
2e	cis−cis−trans	−508.97598
2f	trans−trans−trans	−508.96474
2g	trans−cis−trans	−508.96911
3a	cis−cis−cis	−508.94916
3b	cis−cis−trans	−508.94918
3c	cis−trans−cis	−508.94870
3d	cis−trans−trans	−508.94873
3e	trans−cis−cis	−508.94338
3f	trans−cis−trans	−508.94460
3g	trans−trans−cis	−508.91798
3h	trans−trans−trans	−508.94458
3j	perp−cis−cis	−508.94473
3k	perp−cis−trans	−508.94473
3l	perp−trans−cis	−508.94451
3m	perp−trans−trans	−508.94451
4a	cis−cis	−508.96097
4b	cis−trans	−508.97145
4c	cis−perp	−508.96848
4d	trans−cis	−508.93326
4e	trans−trans	−508.93654
4f	trans−perp	−508.94222
5a	trans−cis	−508.92755
5b	trans−trans	−508.93143
5c	cis−cis	−508.93448
5d	cis−trans	−508.93460
5e	trans−perp	−508.91191
5f	cis−perp	−508.91866

For convenience, we identify the different rotational conformers by their dihedral angles, with the angles 0°, 90°, and 180° designated as cis, perp, and trans, respectively. Protonation of the carbonyl oxygen atom (O_7) creates seven low energy conformers of **2**. The dihedral angles defining these rotomers are $\tau_1(HO_7C_6O_5)$, $\tau_2(O_7C_6O_5O_4)$, and $\tau_3(HC_8C_6O_7)$. The structure of each rotomer was optimized by holding τ_1, τ_2, and τ_3 constant, whereas all other structural parameters were floated. The cis−cis−cis (**2a**) and cis−cis−trans (**2e**) conformers yield the lowest energy structures. The cis−cis−trans

TABLE 3: Ab Initio Vibrational Frequencies for PAN and Various PAN Protomers[a]

molecule	vibrational frequencies (cm^{-1})
PAN (**1**)	43, 80, 95, 97, 314, 331, 371, 494, 578, 612, 720, 726, 807, 837, 979, 1006, 1074, 1191, 1370, 1420, 1497, 1500, 1842, 1908, 3077, 3144, 3187
$PANH^+$ (**2e**)	43, 68, 77, 111, 259, 317, 333, 432, 540, 607, 638, 670, 741, 792, 931, 952, 1046, 1068, 1183, 1373, 1414, 1447, 1470, 1534, 1619, 2020, 3061, 3128, 3193, 3477
$PANH^+$ (**3b**)	11, 45, 60, 107, 146, 191, 209, 286, 389, 404, 426, 456, 622, 706, 786, 907, 995, 1055, 1062, 1373, 1399, 1416, 1430, 1442, 1919, 2350, 2978, 3079, 3116, 3642
$PANH^+$ (**4b**)	19, 54, 72, 132, 150, 194, 219, 318, 321, 457, 567, 308, 309, 664, 903, 977, 1045, 1069, 1292, 1384, 1420, 1469, 1479, 1491, 1703, 2225, 3078, 3151, 3184, 3684
$PANH^+$ (**5d**)	47, 78, 99, 121, 274, 311, 372, 465, 524, 541, 628, 666, 690, 707, 767, 933, 974, 1064, 1097, 1133, 1418, 1456, 1471, 1478, 1873, 2041, 3068, 3142, 3182, 3248

[a] All vibrational frequencies calculated at the B3LYP/6-31G(d) level of theory for the specified structures.

conformer achieves maximum stabilization by orienting the methyl hydrogen trans to the protonated carbonyl group, thereby minimizing the repulsive hydrogen−hydrogen interaction. Rotation of the methyl hydrogen by 180° relative to the carbonyl oxygen atom transforms the cis−cis−trans conformer into the cis−cis−cis structure and destabilizes the energy by 1.5 kJ mol^{-1}. Rotation of the protonating hydrogen on the carbonyl group by 180° transforms the cis−cis−cis conformer into the trans−cis−cis structure and destabilizes the energy by 18 kJ mol^{-1} as a result of breaking the favorable hydrogen bonding interaction between the proton and the nitrate oxygen atom (O_4).

Protonation of the peroxy oxygen atom (O_5) produces twelve low energy conformations of **3**. The dihedral angles $\tau_1(H_9O_5C_6O_7)$, $\tau_2(HC_8C_6O_7)$, and $\tau_3(O_5O_4N_2O_1)$ define these conformers. The results presented in Table 2 show that the cis−cis−cis and cis−cis−trans conformers attain essentially isoenergetic minimum energy structures. These structures emphasize the importance the $\tau_1 - \tau_2 =$ cis−cis conformation in the energy minimization since all other combinations produce significantly high energies. In fact, the orientation of the nitrate group (τ_3) does not alter the total energy once the molecule acquires the favorable $\tau_1 - \tau_2$ geometry.

Protonation of the nitrate oxygen atom (O_4) produces six low energy conformers of protomer **4**. The present calculations were constrained to configurations with a planar $-ONO_2$ group because Smith and Marsden[36] demonstrated that the lowest energy forms of the related molecule CH_3ONO_2 invariably possessed a planar nitrate moiety. Therefore, the dihedral angles $\tau_1(HO_4O_5C_6)$ and $\tau_2(O_7\ C_6\ O_5O_4)$ define the relevant set of conformers. The results given in Table 2 demonstrate that the $\tau_1 =$ cis conformation minimizes the energy of **4** by 70 to 90 kJ mol^{-1}, relative to the $\tau_1 =$ trans or perp orientations. This stabilization results from a favorable hydrogen-bonding interaction with the carbonyl oxygen atom (O_7) similar to that observed in the low energy conformers of **2**.

Protonation of the terminal oxygen atoms of the $-NO_2$ group (O_1 or O_3) produces eight conformers of **5**. The dihedral angles $\tau_1(HO_3N_2O_1)$ and $\tau_2(O_5O_4N_2O_1)$ define these structures. Table 2 presents the energies for six possible combinations of cis, trans, and perp orientations. The cis−cis and cis−trans conformers yield essentially equivalent energy minima, differing in energy by less than 1 kJ mol^{-1}, with the trans−trans conformer lying only 8 kJ mol^{-1} higher in energy. The loss of planarity strongly disfavors any of the structures with perp orientations for either dihedral angle.

TABLE 4: Ab Initio Energies (hartrees) and Proton Affinities (kJ mol^{-1}) for Four $PANH^+$ Protomers

	G2(MP2) 0 K	CBS-4 0 K	CBS-Q 0 K
PAN (**1**)[a]	−508.01459	−508.09171	−508.05587
$PANH^+$ (**2e**)	−508.30167	−508.38217	−508.34178
PA($PANH^+$ (**2e**)) (kJ mol^{-1})	−753.6	−762.4	−750.5
$PANH^+$ (**3b**)	−508.29628	−508.36178	−508.324151
PA($PANH^+$ (**3b**)) (kJ mol^{-1})	−739.4	−708.9	−704.2
$PANH^+$ (**4b**)	−508.31004	−508.38383	−508.35051
PA($PANH^+$ (**4b**)) (kJ mol^{-1})	−775.6	−766.8	−773.4
$PANH^+$ (**5d**)	−508.26958	−508.34755	−508.30786
PA($PANH^+$ (**5d**)) (kJ mol^{-1})	−669.3	−671.6	−661.5

[a] Ref 9.

The total energies for PAN and the four minimum energy $PANH^+$ protomers identified from the conformational analysis have been calculated using the ab initio model chemistries G2(MP2), CBS-4, and CBS-Q. The results are presented in Table 4. It is important to note that the lowest energy $PANH^+$ structure determined at the B3LYP/6-31G(d) level of theory is **2e** not **4b**, but that structure **4b** is approximately 20 kJ mol^{-1} more stable than **2e** in all of the model chemistry calculations. The bond energies associated with the minimum energy dissociation pathways for protomers **2e** and **4b** are compared in Table 5 with the dissociation energies of protonated HNO_3 and protonated CH_3ONO_2. The thermochemical calculations associated with the dissociation of **2e** to yield $CH_3OOH + NO_3^+$ are complicated by the possible formation of $NO_3^+(C_{2v})$ or $NO_3^+(D_{3h})$. A systematic treatment of the NO_3^+ symmetry breaking problem has been presented in a separate paper,[37] and here it is sufficient to note that the C_{2v} structure is predicted to be more stable than the D_{3h} structure for all model chemistry calculations. The discrepancy between the G2(MP2) and CBS-Q calculations arises from the inadequacy of MPn methods to provide an accurate characterization of NO_3^+,[37] and we believe that the CBS-Q energetics present a more accurate picture for this dissociation process.

Discussion

This study continues our efforts to understand the unusual chemistry and molecular properties of peroxyacetyl nitrate. It was motivated by two interesting results from the experimental measurement of the proton affinity of PAN.[5] First, the reported proton affinity, PA(PAN) = −798 ± 12 kJ mol^{-1}, exceeds the typical proton affinity of $RONO_2$ molecules by 50 kJ mol^{-1}.[15−20] Second, the high PA(PAN) value was attributed to protonation of the carbonyl oxygen atom. Both of these conclusions contradict the conventional description of PAN as a nitrate and would indicate that the chemical bonding in PAN differs from previous determinations.[4,11] Additionally, there are well documented experimental difficulties in obtaining accurate proton affinities for nitric acid and its derivatives, especially when bracketing techniques are used.[15−20] The major complication arises from the competition between multiple protomers with comparable thermodynamic stability but markedly different kinetic behavior. The potential for four or more $PANH^+$ protomers to coexist simultaneously in an experiment intended to measure PA(PAN) emphasizes the need to understand the properties of each protomer. Ab initio calculations have played indispensable role in identifying the most stable protomer and the correct proton affinity for other $RONO_2$ molecules[16,17,20] and should provide valuable insights into the protonation chemistry of PAN.

Table 4 summarizes the ab initio energies and proton affinities of four chemically distinguishable $PANH^+$ protomers. Proto-

TABLE 5: Ab Initio Bond Dissociation Energies for Protomers of HNO_3, CH_3ONO_2, and PAN

	G2(MP2)	CBS-4	CBS-Q	CCSD(T)	expt
$[H_2O\cdots NO_2^+]$	−280.83834	−280.87199	−280.86126		
H_2O	−76.33001	−76.34857	−76.33647		
NO_2^+	−204.47987	−204.50161	−204.49645		
$[H_2O\cdots NO_2^+] \rightarrow H_2O + NO_2^+$ (kJ mol^{-1})	74.7	57.3	74.4	72.4[a]	82.0[b]
$[CH_3OH\cdots NO_2^+]$	−320.04518	−320.07929	−320.06834		
CH_3OH	−115.53182	−115.56118	−115.53827		
$[CH_3OH\cdots NO_2^+] \rightarrow CH_3OH + NO_2^+$ (kJ mol^{-1})	87.9	43.3	88.2	82.0[c]	90.0[b]
$PANH^+$ (**4b**) $\equiv [CH_3C(O)OOH\cdots NO_2^+]$	−508.31004	−508.38383	−508.35051		
$CH_3C(O)OOH$	−303.77967	−303.83702	−303.80364		
$[CH_3C(O)OOH\cdots NO_2^+] \rightarrow CH_3C(O)OOH + NO_2^+$ (kJ mol^{-1})	132.6	118.7	132.4		
$PANH^+$ (**2e**)	−508.30167	−508.38217	−508.34178		
CH_3COOH	−228.79542	−228.79541	−228.76564		
NO_3^+ (C_{2v})	−279.45579	−279.45881	−279.45874		
$PANH^+$ (**2e**) $\rightarrow CH_3COOH + NO_3^+$ (C_{2v}) (kJ mol^{-1})	132.4	335.8	308.2		
NO_3^+ (D_{3h})	−279.42371	−279.41497	−279.44525		
$PANH^+$ (**2e**) $\rightarrow CH_3COOH + NO_3^+$ (D_{3h}) (kJ mol^{-1})	216.6	450.9	343.6		

[a] Ref 15. [b] Ref 13. [c] Ref 14.

nation of the nitrate oxygen atom produces the most stable structure (**4b**). Figure 1 illustrates that this structure corresponds to a peracetic acid-nitronium ion complex, $[CH_3C(O)OOH\cdots NO_2^+]$, with a predicted $O_4\cdots NO_2^+$ bond length of 2.5 Å. This result is consistent with the results obtained for all other $RONO_2$ molecules where the most stable protomer also possesses a structure of the form $[ROH\cdots NO_2^+]$.[14−20] The proton affinities calculated from structure **4b** are −775.6 (G2(MP2)), −766.8 (CBS-4), and −773.4 (CBS-Q) kJ mol^{-1}, somewhat higher than the typical PA($RONO_2$) but still 25 kJ mol^{-1} lower than the experimental value reported by Srinivasan et al.[5] The presence of internal hydrogen bonding to the carbonyl oxygen atom contributes to the stability of this structure. The stabilization afforded by the formation of this five-membered ring may facilitate internal hydrogen transfer and promote interconversion between structures **4b** and **2e**.

Protomer **2e**, produced by protonation of the carbonyl oxygen atom, lies only 18.8 kJ mol^{-1} above protomer **4b**, yet **2e** possesses the structural characteristics of a covalently bound molecule and bears little resemblance to the loosely bound ion−molecule complex **4b**. The proton affinities calculated for structure **2e**, −753.6 (G2(MP2)), −762.4 (CBS-4), and −750.5 (CBS-Q) kJ mol^{-1}, clearly disagree with the experimental measurement of PA(PAN) = −798 kJ mol^{-1}.[5] According to the ab initio calculations, protonation at the carbonyl site not only fails to produce the most stable $PANH^+$ protomer, but also results in a CBS-Q proton affinity that is nearly 50 kJ mol^{-1} below the experimental value attributed to this structure. This discrepancy corresponds to more than 4 times the maximum absolute deviation of the CBS-Q method[30] or the experimental measurement[5] and indicates that the experimental PA(PAN) cannot be justified by protonation at the carbonyl oxygen atom.

Surprisingly, protonation of the $-NO_2$ group, structure **5d**, produces the least stable protomer of the four considered here. In fact, the proton affinity for structure **5d** is more than 100 kJ mol^{-1} lower than that of **4b**. Even protonation of the peroxy oxygen atom, structure **3b**, results in a more stable structure than **5d**. The greater stability of **4** compared to **5** is consistent with the results for other nitrates, but the calculated energy difference between the two protomers is a factor of 2 larger than has been observed in other $RONO_2$ systems.[15−17,19,20]

The ion fragmentation patterns exhibited by $PANH^+$ provide important information about the molecular structure of the dominant protomer. Pate et al. originally confirmed the structure of PAN by monitoring the fragment ions produced during chemical ionization mass spectroscopy experiments.[4] Pate et al. found that the $[M + 1]^+$ ion peak at $m/e = 122$ could be produced using protonated methane as the chemical ionization agent; however, the intensity of the $m/e = 122$ peak was dwarfed by peaks at $m/e = 46$ $[NO_2]^+$ and $m/e = 43$ $[CH_3CO]^+$. Pate et al. ascribed these ion peaks to the dissociation pathway

$$PANH^+ \rightarrow CH_3C(O)OOH + [NO_2]^+ \; (m/e = 46) \qquad \text{(R2a)}$$

$$\rightarrow [CH_3CO]^+ \; (m/e = 43) + O_2 + HNO_2 \qquad \text{(R2b)}$$

Switching to protonated i-C_4H_{10} as the chemical ionization agent resulted in a total disappearance of the $[NO_2]^+$ and $[CH_3CO]^+$ ion signals and a spectrum completely dominated by the $PANH^+$ peak at $m/e = 122$.

These results can be understood based on the thermodynamics of the chemical ionization process. When methane is used as the chemical ionization reagent

$$[CH_5]^+ + PAN \rightarrow PANH^+ + CH_4 \qquad \text{(R3)}$$

and $\Delta H_{rxn}^{298\,K} = PA(PAN) - PA(CH_4) = -773.4 - (-543.5) = -229.9$ kJ mol^{-1} where the CBS-Q proton affinity of $PANH^+$ protomer **4b** has been used. When isobutane is employed as the chemical ionization reagent

$$[i\text{-}C_4H_{11}]^+ + PAN \rightarrow PANH^+ + i\text{-}C_4H_{10} \qquad \text{(R4)}$$

$\Delta H_{rxn}^{298\,K} = PA(PAN) - PA(i\text{-}C_4H_{10}) = -773.4 - (-677.8) = -95.6$ kJ mol^{-1}. Table 5 lists the decomposition energies for $PANH^+$ protomers

$$PANH^+ (\mathbf{4b}) \rightarrow CH_3C(O)OOH + NO_2^+ \qquad \Delta H_{CBS\text{-}Q}^{0\,K} = 118 \text{ kJ mol}^{-1} \qquad \text{(R5)}$$

$$PANH^+ (\mathbf{2e}) \rightarrow CH_3COOH + NO_3^+(C_{2v}) \qquad \Delta H_{CBS\text{-}Q}^{0\,K} = 308 \text{ kJ mol}^{-1} \qquad \text{(R6a)}$$

$$PANH^+ (\mathbf{2e}) \rightarrow CH_3COOH + NO_3^+(D_{3h}) \qquad \Delta H_{CBS\text{-}Q}^{0\,K} = 344 \text{ kJ mol}^{-1} \qquad \text{(R6b)}$$

Thus, the proton transfer from CH_5^+ to PAN is sufficiently exothermic to cause the $PANH^+$ (**4b**) to undergo secondary dissociation into peracetic acid and NO_2^+, whereas proton transfer from i-C_4H_{11} is 22.4 kJ mol^{-1} too endothermic to access this channel. We note the use of any other $PANH^+$ protomer in the proton exchange reactions results in lower exothermicities. Additionally, none of these proton-transfer reactions can generate the exothermicity necessary to produce $CH_3COOH + NO_3^+$. The thermodynamic arguments presented here are consistent with the fragmentation patterns observed by Pate et al.[4] and Hansel et al.[7] but disagree with the collision induced dissociation mass spectra observed by Srinivasan et al.[5]

The present study suggests that there are many stable $PANH^+$ protomers that could interfere with experimental attempts to measure PA(PAN) and requires that the experiment be optimized so that only the proton affinity of the most stable protomer is measured. The loosely bound ionic complex **4b** should rapidly transfer NO_2^+ to most reactant partners, rendering bracketing techniques inadequate.[14,15,18−20,38] Such chemistry probably accounts for the discrepancy between the ab initio PA(PAN) value and the value reported by Srinivasan et al.[5] We suggest that competitive displacement reactions, such as the scheme used by Cacace et al. to determine the relative PAs of $HONO_2$ and CH_3ONO_2,[15] will prove to be the most reliable way to measure PA(PAN). The exchange reaction

$$H_2O + [CH_3C(O)OOH\cdots NO_2^+] \rightarrow CH_3C(O)OOH + [HOH\cdots NO_2^+] \quad (R7)$$

initially appears to be the best candidate for obtaining PA(PAN) due to the small difference in PA(PAN) and PA(HNO_3), but Hansel et al. have shown that $PANH^+$ reacts rapidly with H_2O to produce protonated peracetic acid.[7] There appear to be no chemical complications in the system

$$CH_3OH + [CH_3C(O)OOH\cdots NO_2^+] \rightarrow CH_3C(O)OOH + [CH_3OH\cdots NO_2^+] \quad (R8)$$

but the PA difference between PAN and CH_3ONO_2 is about 40 kJ mol^{-1}, so the reaction may not be fast enough to obtain a good equilibrium constant.

Conclusions

The proton affinity of PAN has been investigated using ab initio and density functional methods. Four stable $PANH^+$ protomers were identified, and their minimum energy rotational conformers were determined. The global minimum energy protonated PAN structure corresponds to a peracetic acid-nitronium ion complex, $[CH_3C(O)OOH\cdots NO_2^+]$, consistent with previous experimental and theoretical results for other $RONO_2$ molecules. The CBS-Q proton affinity for this species yields $PA^{0\,K}_{CBS\text{-}Q}(PAN) = -773.4 \pm 10$ kJ mol^{-1}. This value is consistent with the proton affinities observed for other $RONO_2$ molecules,[14−20,38,39] but significantly lower than the $PA^{298\,K}_{expt}(PAN) = -798 \pm 12$ kJ mol^{-1} recently reported.[5] Protonation of the carbonyl oxygen atom yields $PA^{0\,K}_{CBS\text{-}Q}$ (**2e**) $= -750.5 \pm 10$ kJ mol^{-1}, which is also significantly lower than the experimental value and suggests that such a protomer cannot account for the unusually large experimental proton affinity measurement. An accurate experimental PA(PAN) measurement should be possible using the competitive ligand exchange technique introduced by Cacace et al.[15] An accurate value of PA(PAN) and a complete understanding of the chemistry associated with $PANH^+$ protomers will be a crucial part of establishing real time mass spectroscopic detection of this important atmospheric species.

Acknowledgment. The authors thank the NASA Jet Propulsion Laboratory for ample computing resources to conduct this research. The NASA Office of Space Science and Applications sponsors the Jet Propulsion Laboratory Supercomputing Project.

References and Notes

(1) Singh, H. B.; Salas, L. J.; Viezee, W. *Nature* **1986**, *321*, 588.

(2) Roberts, J. M.; Williams, J.; Baumann, K.; Buhr, M. P.; Goldan, P. D.; Holloway, J.; Hubler, G.; Kuster, W. C.; McKeen, S. A.; Ryerson, T. B.; Trainer, M.; Williams, E. J.; Fehsenfeld, F. C.; Bertman, S. B.; Nouaime, G.; Seaver, C.; Grodzinsky, G.; Rogers, M.; Young, V. L. *J. Geophys. Res.* **1998**, *103*, 22 473.

(3) Nouaime, G.; Bertman, S. B.; Seaver, C.; Elyea, D.; Huang, H.; Shepson, P. B.; Starn, T. K.; Riemer, D. D.; Zika, R. G.; Olszyna, K. *J. Geophys. Res.* **1998**, *103*, 22 463.

(4) Pate, C. T.; Sprung, J. L.; Pitts, J. N., Jr. *Org. Mass Spectrom.* **1976**, *11*, 522.

(5) Srinivasan, N.; Cooks, R. G.; Shepson, P. B. *Rap. Commun. Mass. Spectrom.* **1998**, *12*, 328.

(6) Tanimoto, H.; Hirokawa, J.; Kajii, Y.; Akimoto, H. *J. Geophys. Res.* **1999**, *104*, 21 343.

(7) Hansel, A.; Wisthlaer, A. *Geophys. Rev. Lett.* **2000**.

(8) Zabel, F. *Z. Phys. Chem.* **1995**, *188*, 119.

(9) Roberts, J. M.; Bertman, S. B. *Int. J. Chem. Kinet.* **1992**, *24*, 297.

(10) Orlando, J. J.; Tyndall, G. S.; Calvert, J. G. *Atm. Environ. A* **1992**, *26*, 3111.

(11) Miller, C. E.; Lynton, J. I.; Keevil, D. M.; Francisco, J. S. *J. Phys. Chem. A* **1999**, *103*, 11 451.

(12) Mazely, T. L.; Friedl, R. R.; Sander, S. P. *J. Phys. Chem.* **1995**, *99*, 8162.

(13) Mazely, T. L.; Friedl, R. R.; Sander, S. P. *J. Phys. Chem. A* **1997**, *101*, 7090.

(14) Cacace, F.; Attina, M.; DePetris, G.; Speranza, M. *J. Am. Chem. Soc.* **1990**, *112*, 1014.

(15) Cacace, F.; Attina, M.; DePetris, G.; Speranza, M. *J. Am. Chem. Soc.* **1994**, *116*, 6413.

(16) Lee, T. J.; Rice, J. E. *J. Am. Chem. Soc.* **1992**, *114*, 8247.

(17) Lee, T. J.; Rice, J. E. *J. Phys. Chem.* **1992**, *96*, 650.

(18) Sunderlin, L. S.; Squires, R. R. *Chem. Phys. Lett.* **1993**, *212*, 307.

(19) Aschi, M.; Cacace, F.; dePetris, G.; Pepi, F. *J. Phys. Chem.* **1996**, *100*, 16 522.

(20) Aschi, M.; Attina, M.; Cacace, F.; Cartoni, A.; Pepi, F. *Int. J. Mass Spectrom.* **2000**, *196*, 1.

(21) Frisch, M. J.; Trucks, G. W.; Schlegel, H. B.; Scuseria, G. E.; Robb, M. A.; Cheeseman, J. R.; Zakrzewski, V. G.; Montgomery, J. A., Jr.; Stratmann, R. E.; Burant, J. C.; Dapprich, S.; Millam, J. M.; Daniels, A. D.; Kudin, K. N.; Strain, M. C.; Farkas, O.; Tomasi, J.; Barone, V.; Cossi, M.; Cammi, R.; Mennucci, B.; Pomelli, C.; Adamo, C.; Clifford, S.; Ochterski, J.; Petersson, G. A.; Ayala, P. Y.; Cui, Q.; Morokuma, K.; Malick, D. K.; Rabuck, A. D.; Raghavachari, K.; Foresman, J. B.; Cioslowski, J.; Ortiz, J. V.; Stefanov, B. B.; Liu, G.; Liashenko, A.; Piskorz, P.; Komaromi, I.; Gomperts, R.; Martin, R. L.; Fox, D. J.; Keith, T.; Al-Laham, M. A.; Peng, C. Y.; Nanayakkara, A.; Gonzalez, C.; Challacombe, M.; Gill, P. M. W.; Johnson, B. G.; Chen, W.; Wong, M. W.; Andres, J. L.; Head-Gordon, M.; Replogle, E. S.; Pople, J. A. *Gaussian 98*, revision A.7; Gaussian, Inc.: Pittsburgh, PA, 1998.

(22) Becke, A. D. *J. Chem. Phys.* **1993**, *98*, 5648.

(23) Ditchfield, R.; Hehre, W. J.; Pople, J. A. *J. Chem. Phys.* **1971**, *54*, 724.

(24) Hehre, W. J.; Ditchfield, R.; Pople, J. A. *J. Chem. Phys.* **1972**, *56*, 2257.

(25) Hariharan, P. C.; Pople, J. A. *Mol. Phys.* **1974**, *27*, 209.

(26) Gordon, M. S. *Chem. Phys. Lett.* **1980**, *76*, 163.

(27) Hariharan, P. C.; Pople, J. A. *Theor. Chim. Acta* **1973**, *28*, 213.

(28) Frisch, M. J.; Pople, J. A.; Binkley, J. S. *J. Chem. Phys.* **1984**, *80*, 3265.

(29) Clark, T.; Chandrasekhar, J.; Spitznagel, G. W.; von Rague Schleyer, P. *J. Comput. Chem.* **1983**, *4*, 294.

(30) Ochterski, J. W.; Petersson, G. A.; Montgomery, J. A., Jr. *J. Chem. Phys.* **1996**, *104*, 2598.

(31) Curtiss, L. A.; Raghavachari, K.; Trucks, G. W.; Pople, J. A. *J. Chem. Phys.* **1991**, *94*, 7221.

(32) Smith, B. J.; Radom, L. *J. Phys. Chem.* **1995**, *99*, 6468.

(33) Suarez, D.; Sordo, T. L. *J. Phys. Chem. A* **1997**, *101*, 1561.

(34) Del Bene, J. E.; Gwaltney, S. R.; Bartlett, R. J. *J. Phys. Chem. A* **1998**, *102*, 5124.

(35) Lias, S. G.; Bartmess, J. E.; Liebman, J. F.; Holmes, J. L.; Levin, R. D.; Mallard, W. G. *J. Phys. Chem. Ref. Data* **1988**, *17*, 1.

(36) Smith, B. J.; Marsden, C. J. *J. Comput. Chem.* **1991**, *12*, 565.

(37) Miller, C. E.; Francisco, J. S. *J. Phys. Chem. A* **2001**, *105*, in press.

(38) Cacace, F.; DePetris, G.; Pepi, F.; Angelelli, F. *Proc. Natl. Acad. Sci. U.S.A.* **1995**, *92*, 8635.

(39) Lee, T. J.; Rice, J. E. *J. Phys. Chem.* **1993**, *97*, 6637.